Temperature effects on gallium arsenide 63Ni betavoltaic cell

Article (Published Version)

Applied Radiation and Isotopes 125 (2017) 42–47

Contents lists available at ScienceDirect

Applied Radiation and Isotopes

journal homepage: www.elsevier.com/locate/apradiso

Temperature effects on gallium arsenide ^{63}Ni betavoltaic cell

S. Butera*, G. Lioliou, A.M. Barnett

Semiconductor Materials and Devices Laboratory, School of Engineering and Informatics, University of Sussex, Brighton BN1 9QT, UK

ARTICLE INFO

Keywords:
Gallium arsenide
Betavoltaic
Semiconductors

ABSTRACT

A GaAs ^{63}Ni radioisotope betavoltaic cell is reported over the temperature range 70 °C to −20 °C. The temperature effects on the key cell parameters were investigated. The saturation current decreased with decreased temperature; whilst the open circuit voltage, the short circuit current, the maximum power and the internal conversion efficiency values decreased with increased temperature. A maximum output power and an internal conversion efficiency of 1.8 pW (corresponding to 0.3 μW/Ci) and 7% were observed at −20 °C, respectively.

1. Introduction

A wide range of technological areas are undergoing miniaturisation putting increasing demands on their associated power supplies. Microelectromechanical systems (Judy, 2001) are ever decreasing in size requiring similarly shrinking power supplies; reducing power supply weight is vital in lowering the cost and thus increasing the accessibility of space science platforms (Landis et al., 2012). Size is not the sole consideration; replacing spent batteries in implantable medical devices (Lueke and Moussa, 2011), for example, is costly and inconvenient for both patient and healthcare service. In defense applications, FPGA encryption key battery-backed memory needs to be continuously powered since encryption keys are stored in memory systems only as long as energy is supplied to them. Therefore, longevity and durability are also paramount. In some circumstances, chemical or solar batteries are not ideal for these purposes due to their requirement for periodic recharge or replacement, their lack of environmental tolerance, or the need for solar illumination. In long life and harsh environment applications which only require small amounts of power, nuclear microbatteries are becoming increasingly attractive; they also offer useful properties such as high-energy density, and insensitivity to environment and temperature. In nuclear microbatteries, the high-energy particles, released by radioactive atoms during nuclear decay, are absorbed by the microbattery conversion material generating electrical energy (Bower et al., 2002). Recently, a number of alpha, beta and X-ray microbatteries have been reported (Landis et al., 2012; Revankar and Adams, 2014; Butera et al., 2016a, 2016b). Beta emitters, in particular, have received research interest because of their ability to produce relatively high output powers with minimal lattice damage to the conversion device. The use of wide bandgap semiconductors for the conversion material is attractive because of the lower thermally generated leakage currents with respect to narrower badgap semiconductors; moreover, analysis has shown that the efficiency of conversion increases with increased bandgap (Bower et al., 2002). At room temperature, semiconductors such as GaAs, SiC, GaN and diamond have been successfully used as converter materials in betavoltaic cells by several researchers (Chen et al., 2011; Sciuto et al., 2011; Chandrashekhar et al., 2006; Eiting et al., 2006; Cheng et al., 2012; Bormashov et al., 2015). Experimental studies on the temperature effects on betavoltaic batteries have been also carried out, since nuclear microbatteries can be essential in outer space and deep-sea applications. These environments are under high- or low- temperature condition and the temperature can vary over a wide range; hence, the electrical performance of a nuclear microbattery should be analysed under different temperatures. Liu et al. (2012) simulated and tested open circuit voltage (V_{OC}) and short circuit current (I_{SC}) of a betavoltaic cell based on ^{63}Ni-Si as a function of temperature, they found that V_{OC} became highly sensitive to temperature, and the temperature dependence of V_{OC} can be expressed as an exponential function. Wang et al. (2010) studied the relationship between temperature and electrical performance of two ^{63}Ni-Si betavoltaic cells; they proved that the electrical performance such as open circuit voltage (V_{OC}), maximum output power (P_m) and conversion efficiency clearly decreased with increase in temperature: in the temperature range 233.15–333.15 K the changing in values of V_{OC} of the two cells were −3.1 and −3.0 mV/K, these changes resulted in decreased P_m (8.94 nW at 233.15 K, whilst 2.18 nW at 333.15 K for the best beta cell) and conversion efficiency (1.09% at 233.15 K, whilst 0.265% at 333.15 K for the best beta cell), since I_{SC} varied very little with temperature. Chandrashekhar et al. (2007) investigated the change in V_{OC} of a ^{63}Ni-4H SiC betavoltaic cell

* Corresponding author.
E-mail address: S.Butera@sussex.ac.uk (S. Butera).

http://dx.doi.org/10.1016/j.apradiso.2017.04.002
Received 18 October 2016; Received in revised form 23 February 2017; Accepted 1 April 2017
Available online 03 April 2017

in response to temperature; a linear sensitivity of 2.7 mV/K was obtained from 24 to 86 °C. Wang et al. (2015) experimentally and theoretically studied the effect of temperature on the output performance of ^{63}Ni-Si, ^{63}Ni-GaAs, ^{147}Pm-Si, and ^{147}Pm-GaAs microbatteries: in the temperature range 213.15–333.15 K, while the short circuit current (I_{SC}) increased slightly with temperature, the open circuit voltage (V_{OC}) decreased evidently with the increase in temperature and the V_{OC} sensitivities caused by temperature for ^{63}Ni-Si, ^{63}Ni-GaAs, ^{147}Pm-Si, and ^{147}Pm-GaAs microbatteries were −2.57, −5.30, −2.53, and −4.90 mV/K respectively; the conversion efficiency decreased also with the increase in temperature. Tang et al. (2015) demonstrated a radioluminescence nuclear battery that consisted of a ^{147}Pm radioactive isotope, ZnS:Cu phosphor layer and GaAs photovoltaic cell; the effects of temperatures on the microbattery system were studied: experimental and theoretical results indicated that short circuit current density (J_{SC}) slightly decreased with the increase in temperature, whereas open circuit voltage (V_{OC}) and the maximum output power (P_m) rapidly decreased with temperature (dV_{OC}/dT was −3.07 mV/K within the low temperature range of 223.15 K to 303.15 K).

GaAs is a III-V wide bandgap material that can give many advantages in a nuclear microbattery. It can be grown with very high crystal quality, its growth and processing techniques are relatively cheap and more routinely available than some alternative wide bandgap materials providing cost efficiency benefits; for these reasons it has been widely employed in the semiconductor industry, such as in optoelectronic devices and photovoltaic cells. GaAs also shows high resistance to radiation damage which enables operation under illumination from ^{147}Pm. One beta emitting radioisotope often used in betavoltaic microbatteries is ^{63}Ni; it has a half life of ~100 years. The wide availability, the relatively low cost, the reduced device damage risk due its endpoint energy of 66 keV, and the need for only comparatively little shielding to protect users make ^{63}Ni attractive option in a nuclear power supply. This paper reports initial characterisation of a GaAs ^{63}Ni radioisotope beta cell, using a custom GaAs photodiode originally intended for soft X-ray photon counting spectroscopy in space science. Beta particles, emitted by the ^{63}Ni radioisotope beta source, were directly converted into electrical energy using the GaAs device. The effect of temperature on the key parameters of the GaAs ^{63}Ni radioisotope betavoltaic cell were studied over the temperature range 70 °C to −20 °C. This paper differs from previous studies on GaAs ^{63}Ni betavoltaic batteries (Wang et al., 2015) because of the different structure of the GaAs device used and the temperature range studied.

2. Materials and methods

2.1. Radioactive source and energy conversion device

A standard laboratory ^{63}Ni radioisotope beta source was used to illuminate a GaAs energy conversion device. The beta source was positioned as close as experimentally possible (3 mm) to the top of the GaAs device such to minimize the attenuations of the electrons in the dry nitrogen environment of the temperature test chamber which was used to achieve and maintain the temperatures investigated, and inside which the prototype cell was placed. A 400 µm diameter p^+-i- n^+ unpassivated GaAs mesa photodiode was used to collect the electrons emitted by the beta source. The GaAs epilayer of the device was grown to the Authors' specifications by metalorganic vapour phase epitaxy (MOVPE) on a commercial GaAs n^+ substrate at the EPSRC National Centre for III-V Technologies, Sheffield, UK. After growth, the wafer was processed to form mesa structures using wet etching techniques a 1:1:1 H_3PO_4:H_2O_2:H_2O solution was used followed by 10 s in 1:8:80 H_2SO_4:H_2O_2:H_2O solution. The device layers, their relative thicknesses and materials are summarised in Table 1. The p^+-side Ohmic contact covered 33% of the surface of the photodiode studied. Fig. 1 shows schematically the geometry of the ^{63}Ni source and the GaAs detector.

Table 1
Layer details of the GaAs beta-photodiode.

Layer	Material	Thickness (µm)	Dopant	Dopant type	Doping density (cm^{-3})
1	Ti	0.02			
2	Au	0.2			
3	GaAs	0.5	Be	p^+	2×10^{18}
4	GaAs	10	undoped		$<10^{15}$
5	GaAs	1	Si	n^+	2×10^{18}
6	Substrate n^+ GaAs				
7	Au	0.2			
8	InGe	0.02			

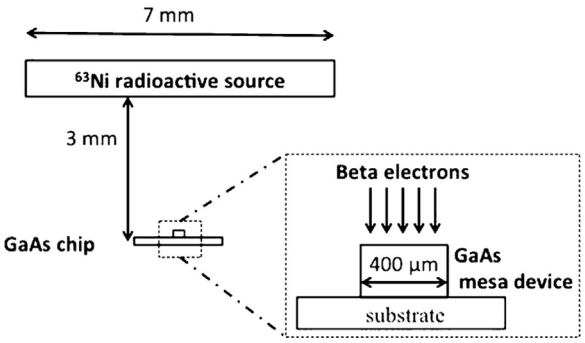

Fig. 1. Schematic geometry of the GaAs ^{63}Ni betavoltaic cell.

The absorption of the beta electrons in the GaAs ^{63}Ni radioisotope betavoltaic cell was studied using the Monte Carlo computer modelling package CASINO (version 3.3) (Hovington et al., 1997; Drouin et al., 1997): CASINO allowed the study of where the beta electrons are absorbed in the GaAs structure. At this stage, we were only interested in quantifying the percentage (*QE*) of the energy of the electrons that were incident on the face of the cell that was absorbed through the GaAs device of specified thickness. Simulations were run such to study the *QE* of the device at each beta electron energy (1–66 keV); each simulation had 4000 beta particles. The source-device geometry was not studied in these particular Monte Carlo simulations. 66 simulations at different beta electron energies were run and the *QE* studied. In each case, (i.e. to determine the cell *QE* for energies from 1 keV to 66 keV in 1 keV steps), the beta particles were simulated as incident on the p^+- side of the GaAs epilayer; thus beta particle absorption through the device thickness studied. The *QE* of the GaAs structure as a function of beta particle energy is shown in Fig. 2.

The simulations also showed that for the particular experimental set

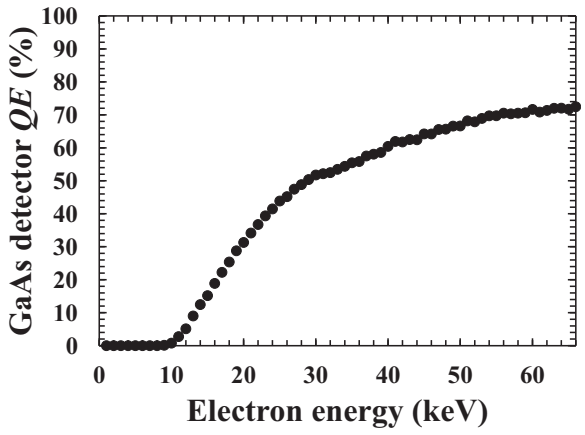

Fig. 2. *QE* of the GaAs structure as a function of the beta electron energy, as determined by Monte Carlo modelling.

up used, beta particles with energies below 25 keV did not reach the GaAs i-layer primarily because of the attenuation of the particles' energies in the protective inactive Ni over-layer (1 μm thick) of the radioisotope beta particle source used. The source had this inactive overlayer for laboratory safety reasons; an eventual real world micro-battery would use a ^{63}Ni radioisotope beta source without such a layer. Attenuation through the top contact (covering 33% of the diode's face) and p^+ layer of the GaAs device was a secondary effect. Beta electrons with energy ≥25 keV deposited part of their energy in the i-layer (e.g. 53% of the energy of the 66 keV electrons was absorbed in the i-layer). The attenuation of the beta particles in the dry nitrogen gap (3 mm) was also investigated with CASINO and found to be negligible compared to the other losses. The emission spectrum of the ^{63}Ni (including beta particle self-absorption in the ^{63}Ni itself) was not taken into account in the simulations; while this was not considered for the calculations of device *QE*, it was essential in the estimation of e.g. the theoretical power, as shown below (Eq. (2)).

In the GaAs ^{63}Ni radioisotope betavoltaic cell, electron-hole pairs were generated in the semiconductor by the beta electrons emitted from the ^{63}Ni radioisotope. The average energy consumed in the generation of an electron-hole pair is called the electron–hole creation energy (4.18 eV for GaAs (Bertuccio and Maiocchi, 2002)). Because of the combination of built-in and applied electric field, the electrons and holes created in the depletion region, and in the n and p regions near the depletion boundary (i.e. closer than the appropriate carrier's diffusion length), accelerate in opposite directions and are swept to the p^+-type and n^+-type regions, respectively, generating a photo-current.

2.2. Experiment and measurements

The GaAs ^{63}Ni radioisotope betavoltaic cell was characterised using a Keithley 6487 picoammeter/voltage source. Forward bias measurements from 0 V to 0.5 V were made in 0.005 V increments in dark conditions and under the illumination of the ^{63}Ni radioisotope beta source. The uncertainty associated with the current readings was 0.3% of their values plus 400 fA, while the uncertainty associated with the applied biases was 0.1% of their values plus 1 mV (Keithley Instruments, 2011). The GaAs ^{63}Ni radioisotope betavoltaic cell was characterised in the temperature range 100 °C to −20 °C. To control the temperature and humidity, the beta cell was placed inside a TAS Micro MT climatic cabinet in a dry nitrogen atmosphere (relative humidity < 5%).

Fig. 3 shows typical dark current characteristics as a function of forward bias at different temperatures for the 400 μm diameter GaAs photodiode. At high temperatures, the dark currents through the

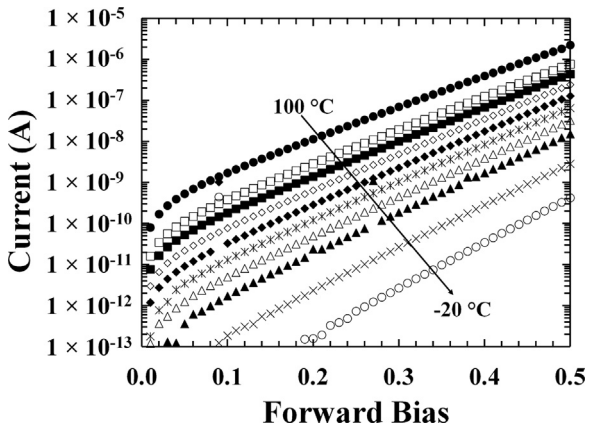

Fig. 3. Dark current as a function of applied forward bias for the 400 μm diameter GaAs photodiode. The temperatures studied were 100 °C (filled circles), 80 °C (empty squares), 70 °C (filled squares), 60 °C (empty rhombuses), 50 °C (filled rhombuses), 40 °C (stars), 30 °C (empty triangles), 20 °C (filled triangles), 0 °C (crosses) and −20 °C (empty circles).

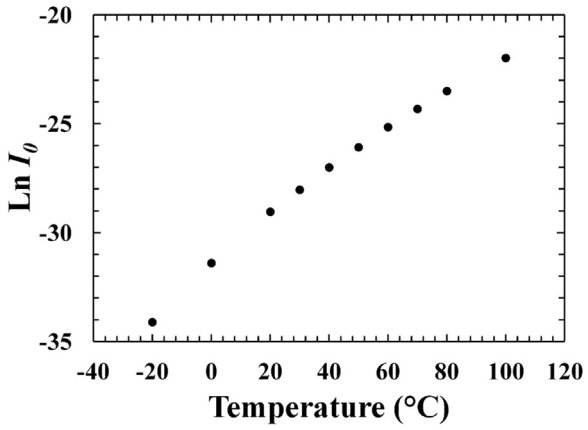

Fig. 4. The logarithm of the saturation current as a function of temperature for the GaAs photodiode.

devices increased due to the greater thermal energy available.

At each temperature, a higher dark current was observed at increased applied biases because of the greater applied electric fields across the photodiode's depletion region. In a simple p-n diode, the dark current increases exponentially as a function of applied bias according Eq. (1),

$$I = I_0 \exp\{qV/nkT\} \quad (1)$$

where n is the ideality factor, k is the Boltzmann constant and T is the temperature (Sze and Ng, 2007). A linear least squares fit of the natural logarithm of the dark current data as a function of applied bias was used to calculate the saturation current (I_0) and the ideality factor (n) of the GaAs device at each temperature: Eq. (1) was linearised as Ln I = A + BV, with A = Ln I_0 and B = q$(nkT)^{-1}$, and used linear least square fitting. Fig. 4 and Fig. 5 show the logarithm of the measured saturation current and the ideality factor as functions of temperature, respectively.

The magnitude of the extrapolated natural logarithm of the saturation current decreased with increasing temperatures was in accordance with Butera et al. (2016a), where a similar GaAs structure was used. On the logarithmic scale in Fig. 4, the observed increase was 12.12 ± 0.02 between 100 °C and −20 °C (corresponding to an increase in saturation current, I_0, of 0.28 pA). This was in remarkable agreement with the expected increase 11.48 (corresponding to an increase in saturation current, I_0, of 0.43 pA), computed using the simple assumption that the temperature dependence of the saturation current was proportional to exp(-$E_g/2kT$) (Butera et al., 2016a). At every temperature, an ideality factor close to 2 was observed; this indicated that generation-recombination current was dominant over the diffusion current in the device in the temperature range studied. The small increase in ideality factor as

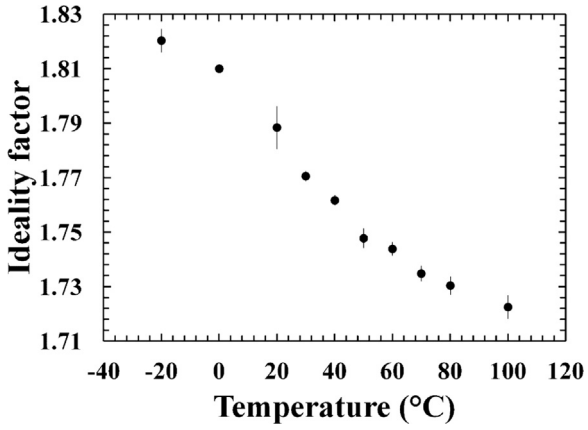

Fig. 5. Ideality factors computed from the measured dark currents as a function of applied forward bias for the GaAs photodiode in the temperature range 100 °C to −20 °C.

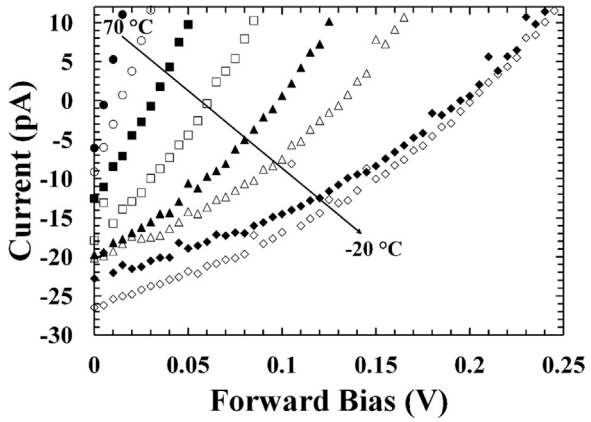

Fig. 6. Current as a function of applied forward bias for the GaAs cell. The temperatures studied were 70 °C (filled circles), 60 °C (empty circles), 50 °C (filled squares), 40 °C (empty squares), 30 °C (filled triangles), 20 °C (empty triangles), 0 °C (filled rhombuses) and −20 °C (empty rhombuses).

the temperature decreased (from 1.723 ± 0.004 to 1.820 ± 0.004 between 100 °C and −20 °C) may be attributed to the decreased contribution of the diffusion current when temperature decreased (Sze and Ng, 2007). A similar behaviour has been previously observed for other GaAs structures (Lioliou et al., 2016).

Under the illumination of the ^{63}Ni radioisotope beta source, the current of the GaAs betavoltaic device was measured as a function of applied bias at different temperatures. From these current characteristics, the experimental values of the open circuit voltage (V_{OC}) were obtained as the interception point of the curves on the horizontal axis. Open circuit voltages higher than 0.005 V were observed at temperatures lower than 70 °C. At temperatures above 70 °C the open circuit voltages were found to be lower than the forward bias step size of 0.005 V, and therefore could not be discriminated; such open circuit voltages have been rounded to zero. Fig. 6 shows the illuminated current characteristics as a function of applied bias between 70 °C and −20 °C. At increased temperature, the softness in the knee of the illuminated current as a function of applied forward bias decreased. At −20 °C, a different behaviour, with respect the trend shown by the other temperatures, was observed: the curve at −20 °C almost overlapped the curve at 0 °C indicating that saturation effects from beta particle induced conduction became dominant over the thermal mechanism at increased forward voltages; the beta electrons, loosing energy through the samples, generated electron-hole pairs along their trajectories that decreased the resistivity in that region. Since the depletion region decreased at increased forward voltages, the percentage of the lower resistivity region in the depletion region increased and the beta induced conductive mechanism was more evident.

Fig. 7 shows the open circuit current as a function of temperature for the GaAs ^{63}Ni radioisotope betavoltaic cell between −70 °C and 20 °C.

The open circuit voltage (V_{OC}) decreased with increased temperature, reaching a saturation value of 0.2 V at −20 °C. Between 70 °C and 0 °C V_{OC} values in accordance with Butera et al. (2016a) (where similar GaAs structure was used) were observed. The dependence of V_{OC} from temperature agreed with other experimental studies reported in literature (Liu et al., 2012; Tang et al., 2015). This behaviour may be explained considering the dependence of the open circuit voltage from the saturation current (Sze and Ng, 2007). Also similarly to Butera et al. (2016a), a linear relationship between the open circuit voltage and temperature was observed at temperatures between 40 °C and 0 °C. In this temperature range, a linear least squares fit showed that V_{OC} was dependent on temperature (T) according the relation $V_{OC} = -AT + B$ with $A = (0.0032 \pm 0.0001)$ V °C^{-1} and $B = (0.192 \pm 0.003)$ V. At −20 °C, in contrast with Butera et al. (2016a), the open circuit voltage appeared to saturate to a value ≈0.2 V; this could be due to the higher carrier

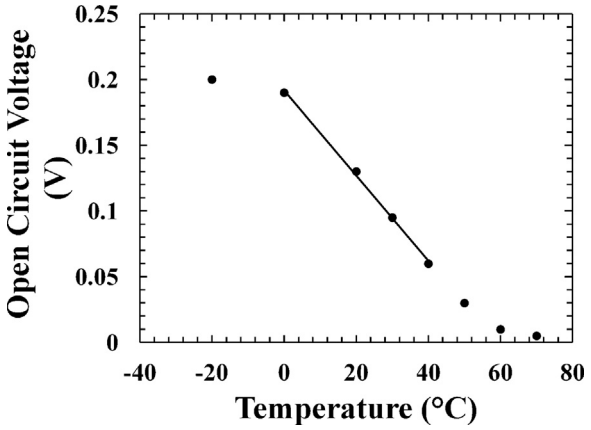

Fig. 7. Open circuit voltage as a function of temperature for the GaAs ^{63}Ni radioisotope beta cell.

density in the semiconductor when it was illuminated with beta electrons compared with X-ray photons previously reported (Butera et al., 2016a). The beta electrons, loosing energy through the samples, generated an increased amount of electron-hole pairs along their trajectories that decreased the material resistivity. The lower resistivity resulted in a lower open circuit voltage compared to Butera et al. (2016a). This mechanism and its effect were evident at low temperature where was dominant over the thermal mechanism. The thermal mechanism consists of the creation of electron-hole pairs due to the thermal energy available. The decrease of the open circuit voltage at increased temperatures for a ^{63}Ni-GaAs betavoltaic battery has been also observed by Wang et al. (2015); V_{OC} temperature dependences of 3.2 mV/°C and 5.30 mV/K were reported here and by Wang (2015), respectively. In Wang et al. (2015), saturation effects are not evident at low temperatures: the open circuit voltage reached a value of ≈0.23 V at −20 °C (similar at the value found here at the same temperature) and continued to increase with decreasing the temperatures.

The experimental values of the short circuit current (I_{SC}) were obtained, at each temperature, as the interception point of the curves in Fig. 6 on vertical axis. Fig. 8 shows the I_{SC} as a function of temperature for the GaAs ^{63}Ni radioisotope betavoltaic cell.

The short circuit current magnitude increased with decreasing temperature, between 70 °C and −20 °C the observed increase was 32.6 pA. This behaviour as a function of temperature has been also observed by other researchers (Butera et al., 2016a; Krawczyk et al., 1981). The dependence of the short circuit current with temperature was instead different from the results reported by Wang et al. (2015) for another ^{63}Ni-GaAs microbattery. In contrast to what is reported here, Wang et al. (2015) found a slightly decrease in the short circuit current

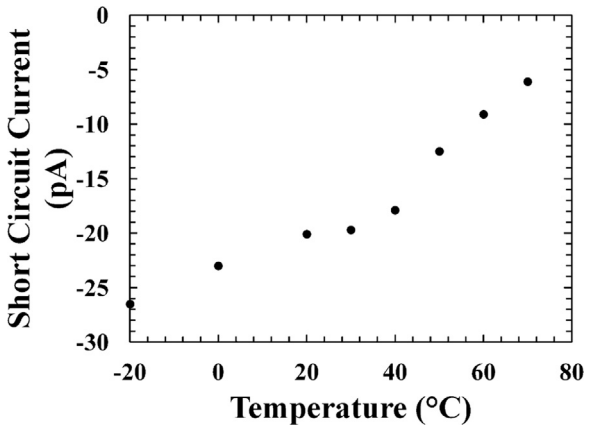

Fig. 8. Short circuit current as a function of temperature for the GaAs ^{63}Ni radioisotope beta cell.

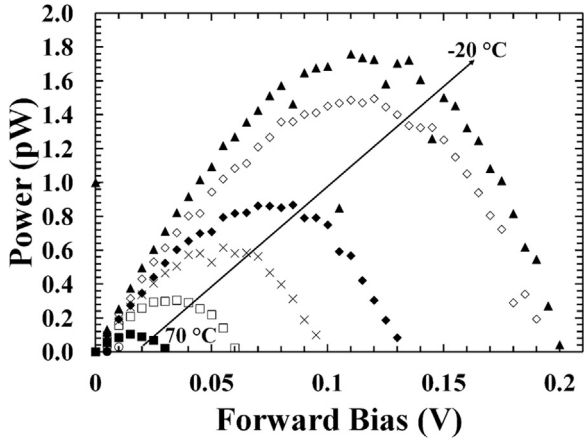

Fig. 9. GaAs ^{63}Ni radioisotope betavoltaic cell output power as a function of applied forward bias at 70 °C (filled circles), 60 °C (empty circles), 50 °C (filled squares), 40 °C (empty squares), 30 °C (crosses), 20 °C (filled rhombuses), 0 °C (empty rhombuses) and −20 °C (filled triangles).

magnitude at decreased temperatures. At −20 °C, a short circuit current density of ≈21 nA/cm^2 was found here, whilst a short circuit current density of ≈11 nA/cm^2 was reported in Wang et al. (2015).

Fig. 9 shows the calculated output power as a function of applied bias for the GaAs ^{63}Ni radioisotope betavoltaic cell at different temperatures. The output power was obtained multiplying the GaAs device current with the corresponding applied bias.

As shown in Fig. 9, the output power increased to a maximum, P_m, and then decreased with increasing applied bias. Fig. 10 shows the maximum output power at each temperature studied.

At decreased temperatures, the maximum output power increased because of its dependence on the open circuit voltage (Sze and Ng, 2007). The determined value of the maximum output power at −20 °C was likely to be an underestimate because of the open circuit voltage measurement previously discussed. A maximum output power as high as 1.8 pW, corresponding to 0.3 μW/Ci (activity associated with decays that produce a beta electron which will strike the detector; the number of electron per second striking the GaAs detector was 5.9×10^{-6} Ci, corresponding to 0.3 μW/Ci (useful activity) (i.e 1.8 pW/5.9×10^{-6} Ci), was observed from the GaAs ^{63}Ni beta radioisotope cell at −20 °C. This value is higher than the maximum output power, observed at −20 °C, by Butera et al. (2016a) (1 pW) using a GaAs ^{55}Fe radioisotope X-ray cell with a similar GaAs converter device. This is mainly due to the higher energy of the beta particles emitted from the ^{63}Ni radioisotope beta source compared with the X-rays emitted from the ^{55}Fe radioisotope X-ray source.

In a more advanced future prototype, a custom interface between the semiconductor converter device and the radioisotope beta particle source will be developed to maximise the proportion of electrons collected by the GaAs device, as well as the fraction of their energy deposited in the i layer (e.g. through the use of a radioisotope beta particle source without a protective inactive Ni overlayer). In the currently reported design, only 0.13% of the beta particles emitted by the radioisotope beta source reached the device, this was in part because of the large area of the ^{63}Ni radioisotope beta particle source (7 mm by 7 mm) compared with the relatively small area of the semiconductor device (400 μm diameter). The stated 0.13% corresponded to the ratio between the number of electrons per second incident on the semiconductor device (2.2×10^5 s^{-1}), and the total number of beta particles per second emitted by the source (1.72×10^8 s^{-1}) after taken into account self-absorption effects (Alam and Pierson, 2016). It has to be noted that in the self-absorption calculation a specific activity of 56 mCi/mg was considered, this value is for a highly pure ^{63}Ni radioactive source (decreased specific activity has to be considered for less pure ^{3}Ni radioactive source); since information about the specific activity of the specific ^{63}Ni source used in the experiment were not available, we made the approximation of having an highly pure ^{3}Ni radioactive source. Of the 1.72×10^8 electrons per second emitted by the ^{63}Ni radioactive source, only half are emitted in the direction down to the plane of the semiconductor device (we assumed that half of the electrons were lost because they were emitted up). The number of electrons per second on the device (2.2×10^5 s^{-1}) was estimated knowing the number of electrons per second emitted downwards by the source towards the plane of the device (8.6×10^7 s^{-1}) and the geometry of the source and detector. The ratio between the area of the device (0.13 mm^2) and the area of the radioactive ^{63}Ni radioisotope beta particle source (49 mm^2) was calculated to be 0.0026. In the above calculation, the simple assumption was made that only beta particles generated in the portion of the area of the source directly above the GaAs device had a possibility of reaching the device.

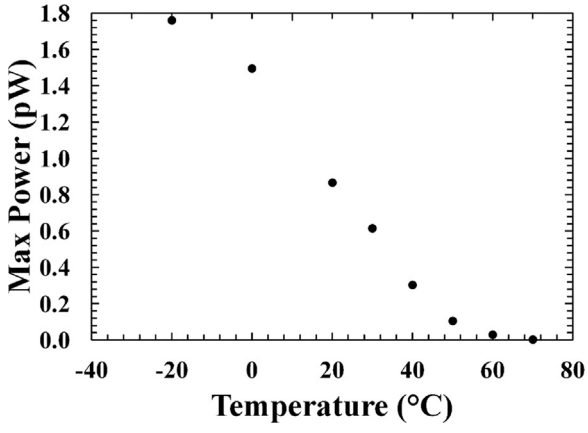

Fig. 10. Experimental maximum power as a function of temperature for the GaAs ^{63}Ni radioisotope betavoltaic cell.

By dividing the maximum measured output power and the maximum power (P_{th}) the cell's internal conversion efficiency was calculated. P_{th} was estimated knowing the source's apparent activity (Alam and Pierson, 2016) and emission probabilities (Preiss et al., 1957), the areas of the ^{63}Ni radioactive source and GaAs mesa device, the percentage of the beta electron energy absorbed in the GaAs device (calculated using CASINO simulations) and the GaAs electron-hole pair creation energy (4.18 eV for GaAs (Bertuccio and Maiocchi, 2002)), according Eq. (2).

$$P_{th} = \sum_{i=0}^{end\ po\ int=66} \frac{A}{2} Em_i \frac{A_{GaAs}}{A_{Ni}} Q\ E_i \frac{i}{\omega_{GaAs}}\ 1.6\cdot10^{-19} \quad (2)$$

where A is the apparent activity of the ^{63}Ni source (172 MBq, under the approximation of an highly pure ^{63}Ni radioactive source), Em_i the emission probability of an electron of energy i, A_{Ni} area of the ^{63}Ni source, A_{GaAs} area of the GaAs detector, QE_i the percentage of each electron energy absorbed in the GaAs device, ω_{GaAs} the GaAs electron-hole pair creation energy. P_{th} was found to be 25 pW.

Fig. 11 shows the calculated internal conversion efficiency (η) as a function of applied bias for the GaAs ^{63}Ni radioisotope betavoltaic cell at different temperatures.

An internal conversion efficiency as high as 7% was observed at −20 °C. This value was calculated as the ration between the maximum output power (P_m) measured at −20 °C and P_{th}. The achieved internal conversion efficiency in the present device was lower than the 9% reported by Butera et al. (2016a) for an X-ray-voltaic cell using similar GaAs structure and an ^{55}Fe radioisotope X-ray source. At each temperature, the internal conversion efficiency was obtained using Eq. (3).

$$\eta = \frac{P_m}{P_{th}} \quad (3)$$

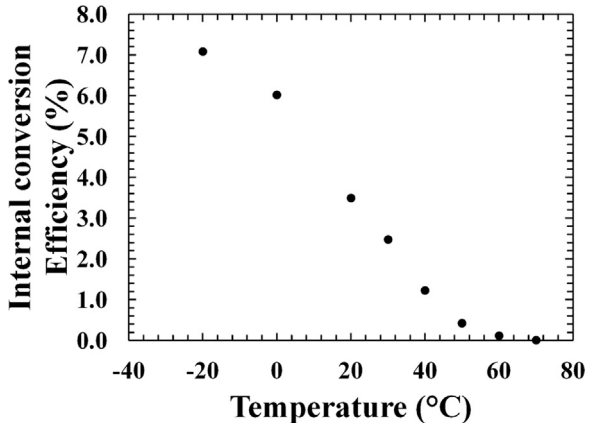

Fig. 11. Internal conversion efficiency (η) as a function of temperature for the GaAs ^{63}Ni radioisotope betavoltaic cell.

where η is the internal conversion efficiency, P_m the maximum experimental output power measured at a particular temperature, and P_{th} the theoretical maximum power obtainable from such system. Slightly higher internal conversion efficiency values would be obtained if we had considered in our calculation a less pure ^{63}Ni radioactive source: in such circumstances the ^{63}Ni specific activity would decrease, thus obtaining a lower P_{th} value and consequently a higher internal conversion efficiency. Considering a specific activity of 11 mCi/mg, an internal conversion efficiency of 9% would have been obtained at −20 °C. It has also to be noted that the overall system efficiency will be much lower than the calculated internal conversion efficiency.

3. Conclusion

In this paper, a prototype GaAs ^{63}Ni radioisotope betavoltaic cell was reported: a ^{63}Ni beta radioisotope was used to illuminate a GaAs converter device such to convert the nuclear energy of the ^{63}Ni beta particle emissions to electrical energy. Using a ^{63}Ni beta radioisotope (activity 185 MBq) ensures a long life microbattery with reduced damage risk for the converter device. GaAs growth and processing techniques are relatively cheap and more routinely available than some alternative wide bandgap materials. Hence the use of GaAs as convert material in the reported prototype may provide cost efficiency benefits in the development of microbatteries for many applications. The custom GaAs photodiode used in the reported betavoltaic cell was originally intended for soft X-ray photon counting spectroscopy in space science. The GaAs ^{63}Ni radioisotope betavoltaic cell was studied between 70 °C and −20 °C, with open circuit voltages lower than the forward bias step size of 0.005 V being observed at temperatures greater than 70 °C. The effect of temperature on the cell's parameters were investigated: while the saturation current increased with increased temperature; the open circuit voltage, the short circuit current, the maximum power and the internal conversion efficiency values increased with decreased temperature. A maximum output power as a high as 1.8 pW (corresponding to 0.3 μW/Ci) was observed at −20 °C. A better microbattery system design that improves the beta particle collection (currently only 0.13% of the beta particles reached the photodiode) could increase the power extracted from the betavoltaic microbattery. An internal conversion efficiency of those beta particles usefully absorbed of 7% was measured at −20 °C.

Data Statement

Data underlying this work are subject to commercially confidentiality. The Authors regret that they cannot grant public requests for further access to any data produced during the study.

Acknowledgments

This work was supported by STFC grant ST/M002772/1 (University of Sussex, A. M. B., PI). The authors are grateful to B. Harrison, R.J. Airey, S. Kumar at the EPSRC National Centre for III-V Technologies for material growth and fabrication. G. Lioliou acknowledges funding received from University of Sussex in the form of a Ph.D. scholarship.

References

Alam, T.R., Pierson, M.A., 2016. Principles of betavoltaic battery design. J. Energy 3, 11.
Bertuccio, G., Maiocchi, D., 2002. Electron-hole pair generation energy in gallium arsenide by x and γ photons. J. Appl. Phys. 92, 1248.
Bormashov, V., Troschiev, S., Volkov, A., Tarelkin, S., Korostylev, E., Golovanov, A., Kuznetsov, M., Teteruk, D., Kornilov, N., Terentiev, S., 2015. Development of nuclear microbattery prototype based on Schottky barrier diamond diodes. Phys. Status Solidi A 212, 2539–2547.
Bower, K.E., Barbanel, Y.A., Shreter, Y.G., Bohnert, G.W., 2002. Polymers, Phosporors, and Voltaics for Radioisotope Microbatteries. CRC Press LLC, Boca Raton.
Butera, S., Lioliou, G., Barnett, A.M., 2016a. Gallium arsenide ^{55}Fe X-ray-photovoltaic battery. J. Appl. Phys. 119, 064504.
Butera, S., Lioliou, G., Krysa, A.B., Barnett, A.M., 2016b. $Al_{0.52}In_{0.48}P$ ^{55}Fe X-ray-photovoltaic battery. J. Phys. D: Appl. Phys. 49, 355601.
Chandrashekhar, M., Duggirala, R., Spencer, M.G., Lal, A., 2007. 4*H* SiC betavoltaic powered temperature transducer. Appl. Phys. Lett. 91, 053511.
Chandrashekhar, M., Thomas, C.I., Li, H., Spencer, M.G., Lal, A., 2006. Demonstration of a 4H SiC betavoltaic cell. Appl. Phys. Lett. 88, 0335061.
Chen, H., Jiang, L., Chen, X., 2011. Design optimization of GaAs betavoltaic batteries. J. Phys. D: Appl. Phys. 44, 215303.
Cheng, Z., Chen, X., San, H., Feng, Z., Liu, B., 2012. A high open-circuit voltage gallium nitride betavoltaic microbattery. J. Micromech. Microeng. 22, 074011.
Drouin, D., Hovington, P., Gauvin, R., 1997. CASINO: a new monte carlo code in C language for electron beam interactions—part II: tabulated values of the mott cross section. Scanning 19, 20–28.
Eiting, C.J., Krishnamoorthy, V., Rodgers, S., George, T., 2006. Demonstration of a radiation resistant, high efficiency SiC betavoltaic. Appl. Phys. Lett. 88, 064101.
Hovington, P., Drouin, D., Gauvin, R., 1997. CASINO: a new Monte Carlo code in C language for electron beam interaction—Part I: description of the program. Scanning 19, 1–14.
Judy, J.W., 2001. Microelectromechanical systems (MEMS): fabrication, design and applications. Smart. Mater. Struct. 10, 1115–1134.
Keithley Instruments, 2011. Inc., Model 6487 Picoammeter/Voltage Source Reference Manual, 6487-901-01 Rev B, Cleveland.
Krawczyk, S., Jakubowski, A., Żurawska, M., 1981. Temperature dependence of the short-circuit current in MIS solar cells. Sol. Cells 4, 187–194.
Landis, G.A., Bailey, S.G., Clark, E.B., Myers, M.G., Piszczor, M.F., Murbach, M.S., 2012. Non-solar photovoltaics for small space missions. In: Proceedings of the 38th IEEE Photovoltaic Specialists Conference, PVSC 2012 (3–8 June 2012), Austin (TX, US), 002819.
Lioliou, G., Meng, X., Ng, J.S., Barnett, A.M., 2016. Characterization of gallium arsenide X-ray mesa p-i-n photodiodes at room temperature. J. Appl. Phys. 813, 1–9.
Liu, Y., Hu, R., Yang, Y., Wang, G., Luo, S., Liu, N., 2012. Investigation on a radiation tolerant betavoltaic battery based on Schottky barrier diode. Appl. Radiat. Isot. 70, 438–441.
Lueke, J., Moussa, W.A., 2011. MEMS-based power generation techniques for implantable biosensing applications. Sensors 11, 1433–1460.
Preiss, I.L., Fink, R.W., Robinson, B.L., 1957. The beta spectrum of carrier-free Ni^{63}. J. Inorg. Nucl. Chem. 4, 233–236.
Revankar, S.T., Adams, T.E., 2014. Advances in betavoltaic power sources. J. Energy Power Sources 1, 321–329.
Sciuto, A., D'Arrigo, G., Roccaforte, F., Mazzillo, M., Spinella, R.C., Raineri, V., 2011. Interdigit 4H-SiC vertical Schottky diode for betavoltaic applications. IEEE Trans. Electron. Dev. 58, 593–599.
Sze, S.M., Ng, K.K., 2007. Physics of Semiconductor Devices, Third ed. John Wiley & Sons, New Jersey.
Tang, X.-B., Hong, L., Xu, Z.-H., Liu, Y.-P., Chen, D., 2015. Temperature effect of a radioluminescent nuclear battery based on 147 Pm/ZnS: Cu/GaAs. Appl. Radiat. Isot. 97, 118–124.
Wang, G., Hu, R., Wei, H., Zhang, H., Yang, Y., Xiong, X., Liu, G., Luo, S., 2010. The effect of temperature changes on electrical performance of the betavoltaic cell. Appl. Radiat. Isot. 68, 2214–2217.
Wang, H., Tang, X.-B., Liu, Y.-P., Xu, Z.-H., Liu, M., Chen, D., 2015. Temperature effect on betavoltaic microbatteries based on Si and GaAs under ^{63}Ni and ^{147}Pm irradiation. Nucl. Instrum. Methods Phys. Res. Sect. B 359, 36–43.